JOURNAL OF Materials CHEMISTRY

Highly non-linear liquid crystal tetramers†

Peter A. Henderson,[a] Rachel T. Inkster,[a] John M. Seddon[b] and Corrie T. Imrie*[a]

[a]*Department of Chemistry, University of Aberdeen, Meston Walk, Old Aberdeen, UK AB24 3UE. E-mail: c.t.imrie@abdn.ac.uk*
[b]*Department of Chemistry, Imperial College of Science, Technology and Medicine, Exhibition Road, London, UK SW7 2AY*

Received 22nd May 2001, Accepted 10th July 2001
First published as an Advance Article on the web 8th October 2001

Three new homologous series of liquid crystal tetramers in which four mesogenic groups are linked *via* three alkyl spacers have been synthesised and characterised. In each series the length of the outer two spacers, *n*, is varied from 3 to 12 methylene units while the central spacer is held at 5 methylene units. The three series differ only in the substitution pattern around the inner two mesogenic units. The series in which the inner spacer is attached to the 4-position on both mesogenic groups is referred to as *n-p5p-n* while *n-p5m-n* refers to attachment at the 4-position on one group and the 3-position on the other. *n-m5m-n* refers to attachment at the 3-position on both groups. All the members of the *n-p5p-n* and *n-p5m-n* series exhibit nematic behaviour. The nematic–isotropic transition temperatures exhibit a pronounced alternation as the length and parity of the outer spacers are varied but which attenuates as *n* is increased. By contrast, the odd–even effects shown by the associated entropy changes are not attenuated as *n* is increased. 4-*p5m*-4 and 5-*p5m*-5 also exhibit smectic behaviour. 4-*m5m*-4 shows a nematic phase and an alternating smectic phase analogous in structure to that observed for certain semi-flexible main chain liquid crystal polymers. The *n-m5m-n* compounds with $n = 6$, 8, 9 and 10 also exhibit a nematic phase and a disordered crystalline phase. The trends in the transitional properties of the series are interpreted in terms of average molecular shapes and a model developed to understand the behaviour of liquid crystal dimers.

Introduction

Low molar mass liquid crystals consisting of bent or banana-shaped molecules have been the subject of considerable research in recent years.[1] Of particular interest has been the observation of new phase structures,[2] ferroelectric and antiferroelectric behaviour[3] and that these achiral molecules can form chiral mesophases.[4] This new field of research in liquid crystal science stems from the first report of such materials by Watanabe and co-workers.[2] Their interest in this novel molecular architecture had been stimulated by their earlier studies of semi-flexible main chain liquid crystal polymers.[5–9] These polymers consist of semirigid mesogenic moieties linked *via* flexible alkyl spacers and the transitional behaviour of such a polymer shows a dramatic dependence on the length and parity of the flexible spacer.[10,11] This is most often attributed to the dependence of the molecular shape on the parity of the spacer considered in the all-*trans* conformation. Specifically, for an even-membered spacer the mesogenic units are antiparallel whereas for an odd-membered spacer they are inclined at some angle with respect to each other. Watanabe and co-workers found that certain odd-membered semi-flexible main chain liquid crystal polymers exhibited novel alternating smectic phases.[5–9] In this phase, the tilt angle alternates between the smectic layers and thus the global tilt angle is zero, but locally within a layer is non-zero. The structural requirement for the observation of this alternation in the tilt direction is simply a correlation of the mesogenic groups which is provided by the flexible spacer and the polymeric nature of the system. The observation of this alternating smectic phase for just bent odd-membered homologues indicated the central role played by molecular shape in phase formation and triggered the development of banana-shaped molecules. Our research, however, focussed on understanding the behaviour of the polymers by studying low molar mass model compounds known as liquid crystal dimers. A liquid crystal dimer consists of molecules containing two mesogenic units linked by a flexible alkyl spacer and their transitional behaviour strongly resembles that of semi-flexible liquid crystal polymers.[12,13] In consequence liquid crystal dimers have been used widely as model compounds for the polymeric systems,[14] although they are now extensively studied in their own right because they exhibit quite different behaviour to conventional low molar mass liquid crystals containing just a single mesogenic unit.[12,13] Liquid crystal dimers also exhibit the novel alternating smectic phase observed for the polymers and again, this has only been observed for bent odd-membered compounds.[15,16] It is thought that the difficulty such bent molecules experience in packing efficiently into the smectic network may provide the driving force for the formation of the alternating smectic phases.

In order to investigate how the transitional properties evolve from the dimers to the polymers, a small number of liquid crystal trimers, consisting of molecules containing three mesogenic groups and two flexible spacers, have been prepared.[17–25] The transitional behaviour of the trimers also strongly resembles that of the polymers although an alternating smectic phase has yet to be observed for a liquid crystal trimer. More recently, we reported the properties of the first homologous series of liquid crystal tetramers in which four mesogenic groups are linked *via* three alkyl spacers.[26] In this particular series the inner flexible spacer was held at eight methylene units while the outer two spacers were varied in length from three to twelve methylene units. The tetramers exhibited an orthogonal smectic phase and this was attributed to the linearity of the central portion of the molecule arising from the even-membered flexible spacer. Here we explore the effects of introducing a non-linear core into a liquid crystal tetramer.

†Basis of a presentation given at Materials Discussion No. 4, 11–14 September 2001, Grasmere, UK.

 DOI: 10.1039/b104490g

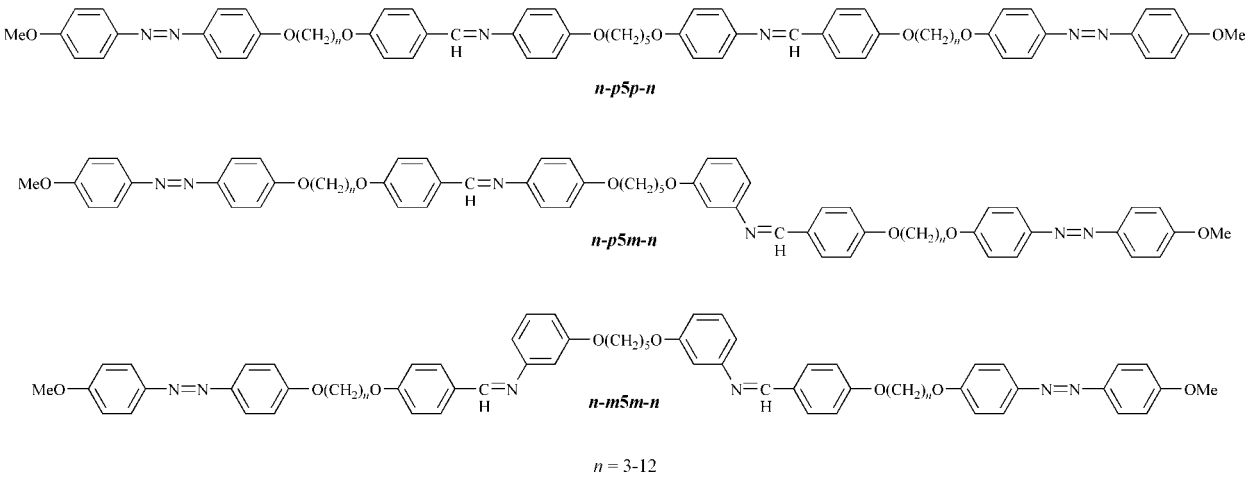

Fig. 1 Molecular structures of the tetramers and the acronyms used to refer to them.

This molecular architecture is realised in two ways: first by having an odd-membered inner flexible spacer and second, by varying the linking position of the inner spacer to the two innermost mesogenic groups. The three liquid crystal tetrameric series studied are shown in Fig. 1 together with the acronyms used to refer to them.

Experimental

Synthesis

The three tetrameric series were prepared using the synthetic route shown in Scheme 1. The syntheses of 4-methoxy-4′-hydroxyazobenzene and the α-bromo-ω-[4-(4-methoxybenzeneazo)phenyloxy]alkanes have been described in detail elsewhere.[27]

α-[4-(4-Methoxybenzeneazo)phenyloxy]-ω-(4-formylphenyloxy)-alkanes, 1. A mixture containing an α-bromo-ω-[4-(4-methoxybenzeneazo)phenyloxy]alkane (10 mmol), 4-hydroxybenzaldehyde (1.34 g, 11 mmol), potassium carbonate (6.91 g, 50 mmol) and DMF (400 mL) was heated at reflux with stirring for six hours. The mixture was cooled and poured into water (400 mL). The resulting yellow precipitate was collected and recrystallised from ethanol.

1, $n = 3$: yield 55%, mp 146 °C. ^{1}H NMR ($CDCl_3$) δ (ppm): 9.9 (s, 1H, CHO), 7.8 (m, 6H, Ar-H), 7.0 (m, 6H. Ar-H), 4.2 (dt, 4H, OCH_2CH_2), 3.9 (s, 1H, OCH_3), 2.3 (quintet, 2H, $CH_2CH_2CH_2$,). IR (KBr) ν (cm^{-1}): 1701 (CO); 841 (*p*-substituted aromatic).

1,5-Bis(4-acetamidophenyloxy)pentane, 2. A mixture containing 1,5-dibromopentane (15.5 g, 0.067 mol), 4-acetamidophenol (21.4 g, 0.142 mol), potassium carbonate (46.3 g, 0.336 mol) and acetone (250 mL) was heated at reflux with stirring overnight. The mixture was cooled and poured into water (1.0 L). The resulting white precipitate was collected and recrystallised from ethanol. The product was too insoluble in any appropriate solvent to allow for structural characterisation using NMR spectroscopy.

Yield 52%, mp 124 °C. IR (KBr): ν (cm^{-1}): 3294 (CONH), 1658 (CO), 830 (*p*-substituted aromatic).

1,5-Bis(4-aminophenyloxy)pentane, 3. A mixture containing **2** (6.50 g, 17 mmol), sodium hydroxide (31.2 g) dissolved in water (35 mL) and ethanol (50 mL) was heated at reflux with stirring overnight. The mixture was cooled and concentrated by rotary evaporation. The resulting mixture was poured into ice–water (100 mL) and the resulting pale brown precipitate recrystallised from ethanol.

Yield 63%, mp 80 °C. ^{1}H NMR ($CDCl_3$) δ (ppm): 6.7 (m, 4H, Ar-H), 6.6 (m, 4H, Ar-H), 3.9 (t, 4H, OCH_2CH_2, J 6.6), 3.3 (s, 4H, ArN-H_2), 1.7 (m, 4H, $CH_2CH_2CH_2CH_2CH_2$), 1.5 (m, 2H, $CH_2CH_2CH_2CH_2CH_2$,). IR (KBr) ν (cm^{-1}): 3432, 3352 (aromatic NH_2); 841 (*p*-substituted aromatic).

1,5-Bis(3-acetamidophenyloxy)pentane 7. Compound **7** was synthesised using the procedure described for **2** except that 3-acetamidophenol was used. Mp 186–187 °C. IR (KBr): ν (cm^{-1}): 3299 (CONH), 1657 (CO), 786 (*m*-substituted aromatic).

1,5-Bis(3-aminophenyloxy)pentane 8. Compound **7** was hydrolysed using the procedure described for **3** to yield **8**. Mp 120 °C. ^{1}H NMR ($CDCl_3$) δ (ppm): 7.0 (t, 2H, Ar-H *ortho* to NH_2 and OCH_2), 6.3–6.2 (m, 6H, Ar-H), 3.9 (t, 4H, OCH_2CH_2, $J = 6.6$), 3.6 (s, 4H, ArN-H_2), 1.8 (m, 4H, $CH_2CH_2CH_2CH_2CH_2$), 1.6 (m, 2H, $CH_2CH_2CH_2CH_2CH_2$,). IR (KBr) ν (cm^{-1}): 3403, 3307 (aromatic NH_2).

1-(4-Acetamidophenyloxy)-5-bromopentane, 4. A mixture containing 1,5-dibromopentane (91.9 g, 0.40 mol), 4-acetamidophenol (6.05 g, 0.040 mol), potassium carbonate (27.6 g, 0.20 mol) and acetone (100 mL) was heated at reflux with stirring overnight. The mixture was filtered hot, the filtrate collected, and the acetone removed by rotary evaporation. The remaining liquid was poured into 40–60 °C petroleum spirit (200 mL). The resulting white precipitate was collected and recrystallised from ethanol.

Yield 56%, mp 119–121 °C. ^{1}H NMR ($CDCl_3$) δ (ppm): 7.3 (d, 2H, Ar-H, $J = 9.0$), 6.8 (d, 2H, Ar-H, $J = 9.0$), 3.9 (t, 2H, OCH_2CH_2, $J = 6.0$), 3.4 (t, 2H, $BrCH_2CH_2$, $J = 6.8$), 2.1 (s, 3H, CH_3CO), 1.9 (quintet, 2H, $CH_2CH_2CH_2$, $J = 7.0$), 1.8 (m, 2H, $CH_2CH_2CH_2$), 1.6 (m, 2H, $CH_2CH_2CH_2$). IR (KBr) ν (cm^{-1}): 3298, 3258, 1657 (CONH); 830 (*p*-substituted aromatic).

1-(4-Acetamidophenyloxy)-5-(3-acetamidophenyloxy)pentane, 5. A mixture containing **4** (6.00 g, 0.020 mol), 3-acetamidophenol (3.63 g, 0.024 mol), potassium carbonate (13.82 g, 0.10 mol) and acetone (100 mL) was heated at reflux with stirring overnight. The mixture was cooled and poured into water (700 mL). The resulting white precipitate was collected and recrystallised from ethanol.

Yield 68%, mp 129–130 °C. IR (KBr) ν (cm^{-1}): 3408, 3282, 1662 (CONH); 830 (*p*-substituted aromatic).

1-(4-Aminophenyloxy)-5-(3-aminophenyloxy)pentane, 6. A mixture containing **5** (4.80 g, 0.013 mol), sodium hydroxide

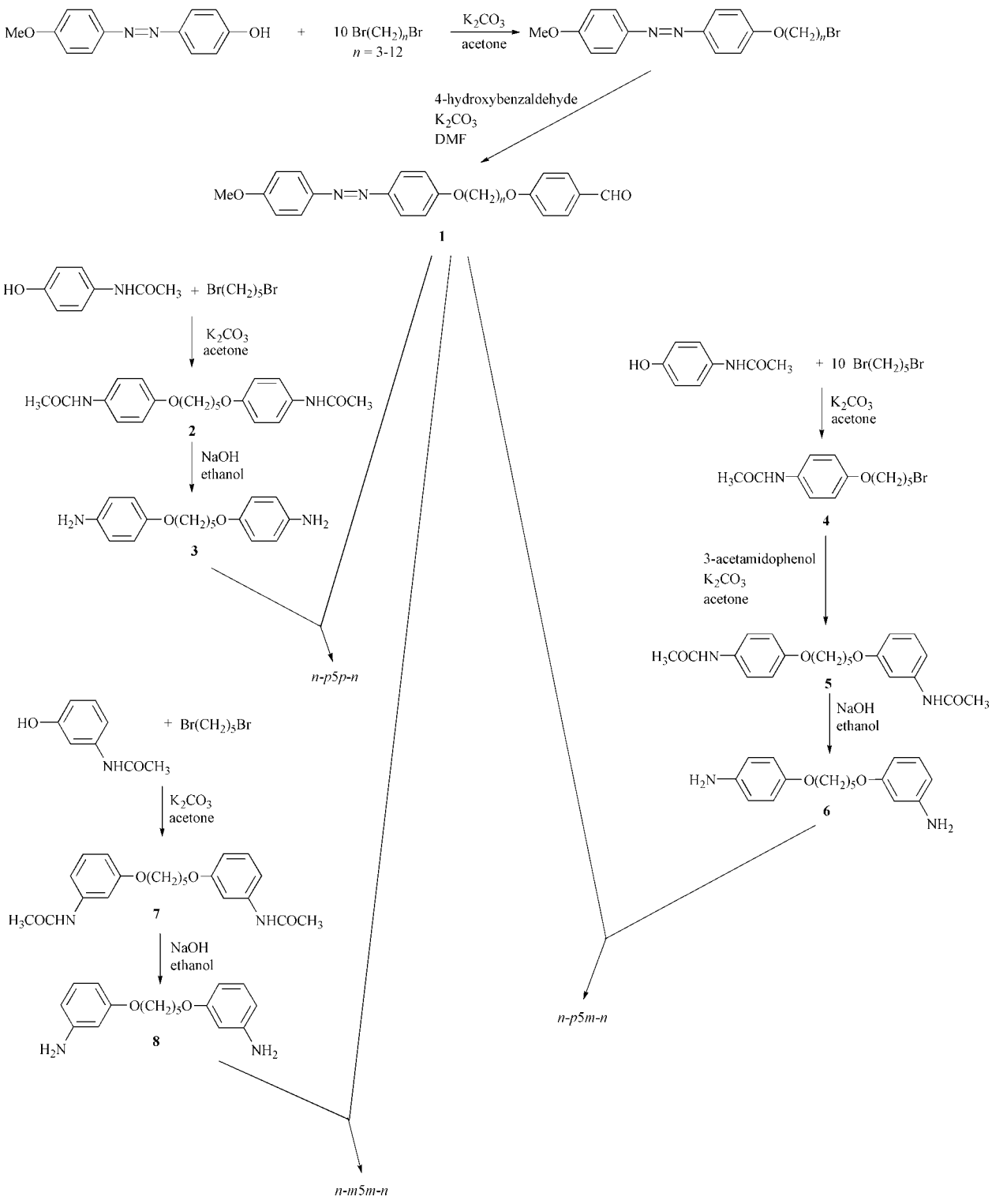

Scheme 1

(23.3 g) dissolved in water (35 mL) and ethanol (80 mL) was heated at reflux with stirring overnight. The mixture was cooled and concentrated by rotary evaporation. The mixture was then poured into ice–water (400 mL) and the resulting white precipitate recrystallised from ethanol.

Yield 58%, mp 88 °C. ^{1}H NMR ($CDCl_3$) δ (ppm): 7.0 (t, 1H, Ar-H *ortho* to NH_2 and OCH_2), 6.7 (d, 2H, Ar-H on *para* ring, J = 8.8), 6.6 (d, 2H, Ar-H on *para* ring, J = 8.8), 6.3–6.2 (m, 3H, Ar-H on *meta* ring) 3.9 (dt, 4H, OCH_2CH_2,), 3.5 (s, 4H, $ArNH_2$), 1.8 (m, 4H, $CH_2CH_2CH_2CH_2CH_2$), 1.6 (m, 2H, $CH_2CH_2CH_2CH_2CH_2$,). IR (KBr) ν (cm^{-1}): 3424, 3406, 3350, 3332 (*ortho* and *para* aromatic NH_2).

Tetramers. A representative method is described for 3-*p*5*m*-3. Thus, a mixture containing **6** (0.100 g, 0.35 mmol), 1-[4-(4-methoxybenzeneazo)phenyloxy]-3-(4-formylphenyloxy)propane (0.289 g, 0.74 mmol), a few crystals of toluene-4-sulfonic acid and ethanol (50 mL) was heated at reflux with stirring for 6 hours. The mixture was filtered hot and the resulting yellow residue recrystallised from toluene.

Yield 71%. ^{1}H NMR ($CDCl_3$) δ (ppm): 8.4 (2s, 2H, C*H*N), 7.9–7.8 (m, 12H, Ar-H), 7.2 (m, 2H, Ar-H), 7.0–6.9 (m, 12H, Ar-H), 6.9–6.8 (m, 2H, Ar-H), 6.8–6.7 (m, 4H, Ar-H), 4.3–4.2 (t, 8H, OCH_2CH_2, J = 5.9), 4.1–4.0 (m, 4H, OCH_2CH_2,), 3.85 (s, 6H, OCH_3), 2.4–2.3 (quintet, 4H, $OCH_2CH_2CH_2O$), 1.9–1.8

(quintet, 4H, $CH_2CH_2CH_2CH_2CH_2CH_2$), 1.7–1.6 (m, 2H, CH_2-$CH_2CH_2CH_2CH_2CH_2$,). IR (KBr) ν (cm^{-1}): 1601 (CHN); no NH_2 peaks are present. Anal: calc. for $C_{63}H_{62}N_6O_8$, C 73.13, H 6.06, N 8.15; found, C 73.29, H 6.11, N 8.17%.

All the members of the *n-p5p-n* series were recrystallised from DMF, the *n-m5m-n* series from ethyl acetate and the *n-p5m-n* series from toluene. Products were obtained in yields of 50–80%. The members of the *n-p5p-n* series were too insoluble in any appropriate solvent to allow for structural characterisation using NMR spectroscopy. Their IR spectra, however, were consistent with the proposed structures. Specifically, the bands associated with the stretch and bend deformations of the N–H bond in **3** and that associated with the carbonyl band in **1** are absent in the spectra of the products. In addition elemental analysis data are consistent with the proposed structures and representative data are provided.

3-*p5p*-3: Anal: calc. for $C_{63}H_{62}N_6O_8$, C 73.13, H 6.06, N 8.15; found, C 73.13, H 6.16, N 8.18%.

3-*m5m*-3: ^{1}H NMR ($CDCl_3$) δ (ppm): 8.35 (s, 2H, C*H*N), 7.9–7.8 (m, 12H, Ar-H), 7.0–6.9 (m, 12H, Ar-H), 6.8–6.7 (m, 8H, *meta*-substituted Ar-H), 4.3–4.2 (t, 8H, OCH_2CH_2 J = 5.9), 4.0 (t, 4H, OCH_2CH_2 on *meta*-substituted rings, J 6.3) 3.9 (s, 6H, OCH_3), 2.4–2.2 (quintet, 4H, $OCH_2CH_2CH_2O$), 1.9–1.8 (quintet, 4H, $CH_2CH_2CH_2CH_2CH_2CH_2$), 1.7–1.6 (m, 2H, $CH_2CH_2CH_2CH_2CH_2CH_2$,). Anal: calc. for $C_{63}H_{62}N_6O_8$, C 73.13, H 6.06, N 8.15; found, C 73.23, H 6.15, N 7.98%.

Characterisation

The proposed structures of all the tetramers and their intermediates were verified by a combination of ^{1}NMR spectroscopy, where possible, using a Bruker AC-F 250 MHz spectrometer, and FTIR spectroscopy using an ATI Mattson Genesis FTIR spectrometer.

Thermal characterisation

The thermal properties of the tetramers were determined by differential scanning calorimetry (DSC) using a Mettler Toledo DSC 820 differential scanning calorimeter equipped with a TS0801RO sample robot and calibrated using indium and zinc standards. The heating profile in all cases was heat, cool and reheat at 10 °C min^{-1} with a 3 min isotherm between heating and cooling segments. Phase identification was performed by polarised light microscopy using an Olympus BH-2 optical microscope equipped with a Linkam THMS 600 heating stage and a TMS 91 control unit. X-Ray diffraction patterns were recorded using a Guinier camera fitted with a bent quartz monochromator (R. Huber, Germany) set to isolate Cu-Kα1 radiation (λ = 1.5405 Å) with non-aligned samples held in a thermostatted sample holder.

Results and discussion

n-p5p-n series

The transition temperatures and associated entropy changes exhibited by the *n-p5p-n* series are listed in Table 1. The data were extracted from the reheat DSC traces and a representative trace for 5-*p5p*-5 is shown in Fig. 2. All ten members of the series exhibit nematic behaviour although 12-*p5p*-12 is a monotropic nematogen. Nematic phases were assigned on the basis of the schlieren optical texture containing both two and four brush point singularities when viewed through a polarised light microscope.

The dependence of the transition temperatures on the number of methylene units, n, in the outer flexible alkyl spacers for the *n-p5p-n* series is shown in Fig. 3. The melting points show a marked alteration on varying the parity of n in which the even members have the higher values. This odd–even effect appears not to attenuate on increasing n. The nematic–isotropic transition temperatures also exhibit a pronounced alternation as the length and parity of the outer spacers are varied although this is attenuated on increasing n. For the members having an even value of n, T_{NI} decreases on increasing n whereas for odd members, T_{NI} is much less sensitive to changes in spacer length and passes through a maximum on increasing n. The behaviour seen in Fig. 3 is very similar to that reported on varying the length and parity of the outer spacers in a liquid crystal tetramer series possessing an inner spacer containing an even number of methylene units[26] although the attenuation of the odd–even effect exhibited by T_{NI} is more pronounced for the *n-p5p-n* series. It is interesting to note that the *n-p5p-n* series is exclusively nematogenic and increasing the spacer length has not resulted in smectic phase formation. This is similar to the behaviour observed for liquid crystal trimers[24] and symmetric dimers[28] but quite unlike that of semi-flexible main chain polymers for which increasing

Table 1 Transition temperatures and associated entropy changes for the *n-p5p-n* series. Monotropic transition temperatures are given in parentheses

n	T_{Cr-}/°C	T_{NI}/°C	ΔS_{Cr-}/R	ΔS_{NI}/R
3	208	241	29.6	1.28
4	252	308	29.6	3.84
5	211	244	29.8	1.82
6	232	272	29.5	3.65
7	195	231	26.2	2.00
8	222	248	37.8	4.01
9	190	224	33.0	2.49
10	213	222	32.2	3.42
11	184	211	34.0	2.58
12	208	(205)	50.2	3.90

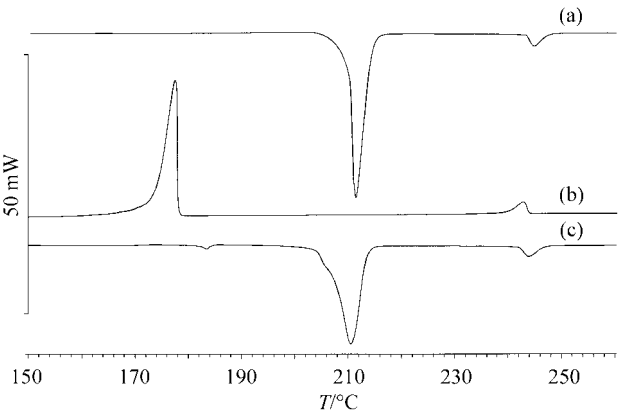

Fig. 2 DSC trace for 5-*p5p*-5: (a) initial heat, (b) cooling and (c) reheat.

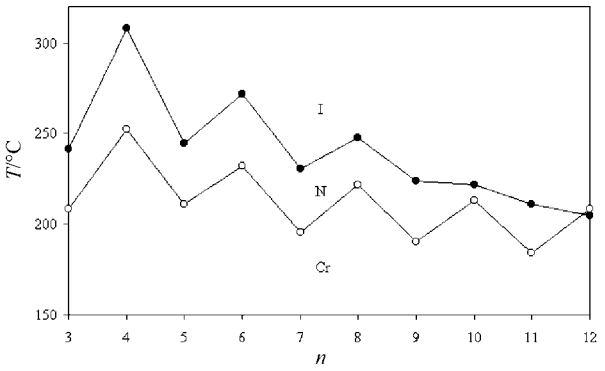

Fig. 3 The dependence of the transition temperatures on the number of methylene units, n, in the outer flexible alkyl spacers for *n-p5p-n*. ○ indicates the melting point and ● the nematic–isotropic transition temperature.

spacer length enhances smectic behaviour.[10,11] Thus, the driving force for smectic phase formation must differ between liquid crystal oligomers and polymers. Presumably for the polymers the driving force must be an entropic one in order to disentangle the polymer chains. The situation is somewhat different for other liquid crystal tetramers for which smectic phase stability does not simply increase or decrease on increasing the length of the outer spacers but for that series the driving force for smectic phase formation was believed to be a specific interaction between the unlike mesogenic groups in the tetramer.[26] For the *n*-*p*5*p*-*n* series such interactions do not exist.

The entropy change associated with the nematic–isotropic transition, expressed as the dimensionless quantity $\Delta S_{NI}/R$, for the *n*-*p*5*p*-*n* series also exhibits a dramatic alternation as *n* is increased (Fig. 4), in which the values of $\Delta S_{NI}/R$ for compounds having an even value of *n* are typically twice those of the odd members. The value of $\Delta S_{NI}/R$ for 10-*p*5*p*-10 appears to be somewhat lower than expected and this may be a result of the close proximity of the melting and clearing transitions leading to an underestimation of $\Delta S_{NI}/R$. The value of $\Delta S_{NI}/R$ for members having even values of *n* are lower than those of tetramers in which all three spacers contain an even number of methylene units.[26] We will discuss the significance of these observations later.

n-*p*5*m*-*n* series

The transition temperatures and associated entropy changes shown by the *n*-*p*5*m*-*n* series are listed in Table 2, and again these data have been extracted from reheat DSC traces. Several members of this series show complex crystallisation and melting behaviour and only the melting point for the highest melting modification is given; a representative DSC trace is shown for 5-*p*5*m*-5 in Fig. 5. All the members of the series exhibit nematic behaviour although 10-*p*5*m*-10 is monotropic in nature. In addition, on cooling the nematic phase of 4-*p*5*m*-4 and 5-*p*5*m*-5, the schlieren texture (Fig. 6(a)) changed to give a truncated fan texture (Fig. 6(b)) when viewed through the polarised light microscope. The strongly monotropic nature of the smectic phase precluded the possibility of X-ray diffraction studies in order to determine the layer spacings. The phase is tentatively assigned as a smectic A phase and the values of the entropy change at the smectic–nematic transition, $\Delta S_{SmN}/R$, support this view. For 4-*p*5*m*-5 $\Delta S_{SmN}/R$ has a value of 0.04 and for 5-*p*5*m*-5 is essentially zero (see Fig. 5). Such low values are to be expected because it is known that $\Delta S_{SmAN}/R$ depends on the length of the preceding nematic range. In fact, $\Delta S_{SmAN}/R$ is observed and predicted to decrease as the ratio of the transition temperatures, T_{SmAN}/T_{NI}, deviates from unity and as

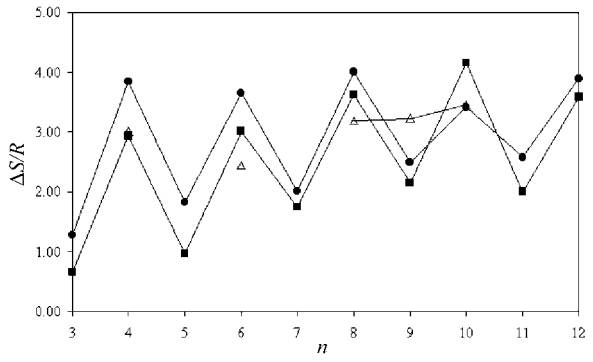

Fig. 4 The dependence of the entropy change associated with the clearing transition on the number of methylene units, *n*, in the outer flexible spacers for the *n*-*p*5*p*-*n* series (●), the *n*-*p*5*m*-*n* series (■) and the *n*-*m*5*m*-*n* series (△). Filled symbols indicate nematic–isotropic transitions and open symbols indicate combined mesophase–nematic–isotropic transitions.

Table 2 Transition temperatures and associated entropy changes for the *n*-*p*5*m*-*n* series. Monotropic transition temperatures are given in parentheses

n	T_{Cr-}/°C	T_{NI}, T_{SmN}[a]/°C	$\Delta S_{Cr-}/R$	$\Delta S_{NI}/R$, $\Delta S_{SmN}/R$[a]
3	150	162	18.2	0.66
4	194	240, (167)[a]	14.4	2.93, 0.04[a]
5	143	173, (87)[a]	16.8	0.97, ~0[a]
6	175	206	16.0	3.01
7	142	175	25.1	1.75
8	146	175	17.6	3.62
9	137	170	26.8	2.16
10	166	(164)	23.9	4.16
11	143	158	9.6	2.00
12	144	147	24.5	3.59

[a]The superscript *a* shows which entries refer to which of the column headings.

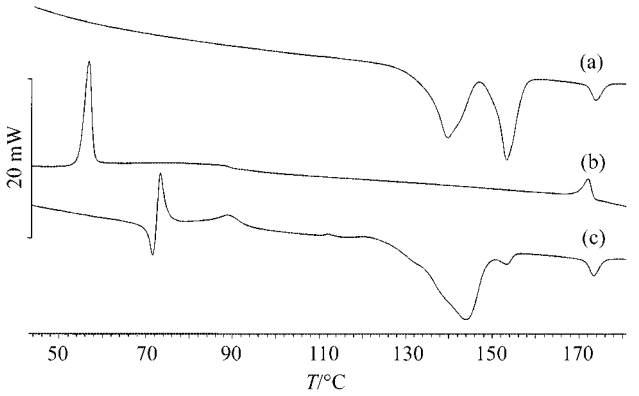

Fig. 5 DSC trace for 5-*p*5*m*-5: (a) initial heat, (b) cooling and (c) reheat.

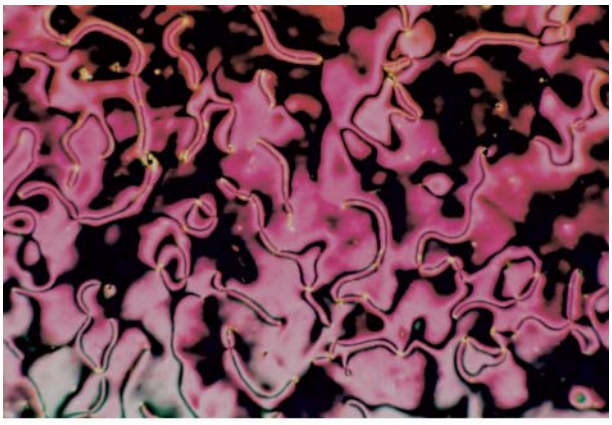

Fig. 6 The optical textures exhibited by 4-*p*5*m*-4: (a) the nematic schlieren texture (239 °C) and (b) the smectic truncated fan texture (164 °C).

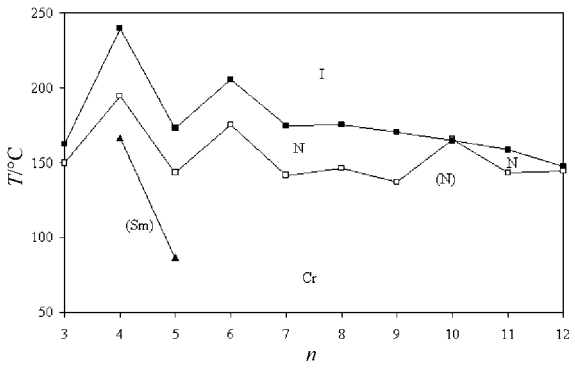

Fig. 7 The dependence of the transition temperatures on the number of methylene units, *n*, in the outer flexible alkyl spacers for the *n*-*p*5*m*-*n* series. □ indicates the melting point, ■ the nematic–isotropic and ▲ the smectic–nematic transition temperatures.

this ratio decreases so the transitional entropy decreases until a critical point is reached at which the transition is second order.[29] For 4-*p*5*m*-4 T_{SmAN}/T_{NI} has a value of 0.86 and for 5-*p*5*m*-5 is 0.81 and hence, the transition entropy is predicted and observed to be small, apparently second order for 5-*p*5*m*-5. We note, however, that the truncated apperance of the fans normally indicates out-of-plane correlations suggesting a more highly ordered phase, a view not supported by the small transition entropy. The absence of smectic behaviour for the higher homologues in the *n*-*p*5*m*-*n* series indicates that increasing spacer length promotes nematic rather than smectic phase behaviour. It is difficult to comment on the significance of this observation without a knowledge of the local organisation of the molecules within the phase.

Fig. 7 shows the dependence of the transition temperatures on the number of methylene units, *n*, in the outer flexible alkyl spacers for the *n*-*p*5*m*-*n* series. The melting points exhibit a pronounced alternation in which even members have the higher values but which is attenuated on increasing *n*. The melting point of 8-*p*5*m*-8 is lower than expected. The nematic–isotropic transition temperatures initially show a marked odd–even effect again in which even members have the higher values but which is rapidly attenuated at 7-*p*5*m*-7. This attenuation reflects a decrease in T_{NI} for members having an even value of *n* on increasing *n* whereas for odd members T_{NI} is much less sensitive to changes in *n* and in fact, passes through a shallow maximum on increasing *n*.

The dependence of the nematic–isotropic entropies on the number of methylene units, *n*, in the outer flexible alkyl spacers of the *n*-*p*5*m*-*n* series is shown in Fig. 4. Again a pronounced alternation is observed on increasing *n* in which even members typically exhibit values of $\Delta S_{NI}/R$ 2–3 times larger than those shown by the odd members. The odd–even effect is not attenuated on increasing *n* although it may be argued that it is attenuated in a relative sense since the values of $\Delta S_{NI}/R$ tend to increase with increasing *n* but the difference between the *n* and $(n + 1)$ homologues appears to be approximately constant.

n-*m*5*m*-*n* series

The transition temperatures and associated entropy changes for the *n*-*m*5*m*-*n* series are listed in Table 3. As with the *n*-*p*5*m*-*n* series several members exhibit complex crystallisation and melting behaviour; see, for example, the DSC trace for 6-*m*5*m*-6 shown in Fig. 8; only data associated with the highest temperature melting transition are given. Five members of the series exhibit liquid crystalline behaviour. On cooling the isotropic phase of 4-*m*5*m*-4, a nematic texture develops which changes immediately to give coexisting regions of rather rounded focal-conic fan and schlieren textures, see Fig. 9. The schlieren texture appears to contain both types of point

Table 3 Transition temperatures and associated entropy changes for the *n*-*m*5*m*-*n* series. Monotropic transitions are given in parentheses. M denotes an unidentified mesophase

n	T_{Cr-}/°C	T_{MNI}/°C	$\Delta S_{Cr-}/R$	$\Delta S_{MNI}/R$
3	138	—	18.1	—
4	169	(163)	24.0	3.01
5	130	—	13.1	—
6	145	150	15.3	2.44
7	124	—	21.1	—
8	136	(131)	24.7	3.20
9	108	(96)	19.6	3.23
10	135	(120)	28.5	3.46
11	115	—	9.9	—
12	138	—	31.2	—

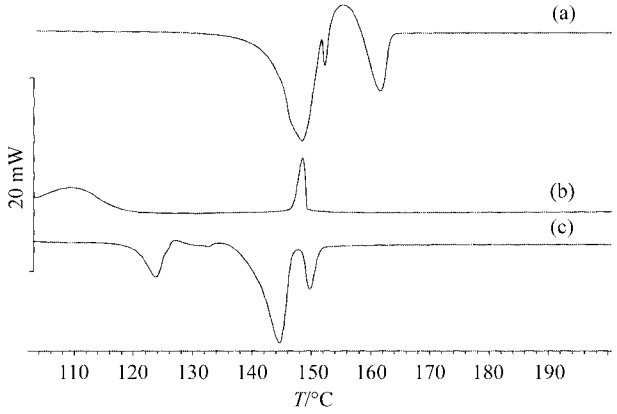

Fig. 8 DSC trace for 6-*m*5*m*-6: (a) initial heat, (b) cooling and (c) reheat.

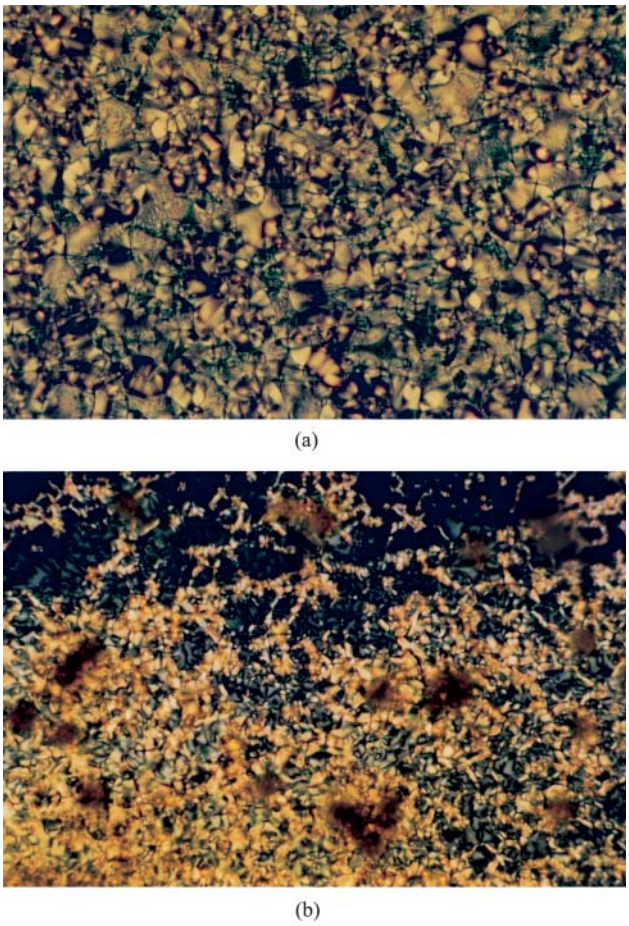

Fig. 9 (a) The focal-conic fan (154 °C) and (b) schlieren (110 °C) textures of the smectic phase exhibited by 4-*m*5*m*-4.

singularity which would normally be thought of to imply a nematic phase. This assignment is in conflict, however, with the observation of coexisting regions of focal-conic fan texture which indicates that the structure is layered. It has been shown, however, that a particular modification of the smectic C phase in which the sense of the tilt angle alternates between adjacent layers exhibits a schlieren texture containing both types of point singularity.[30] As we noted in the introduction, this alternating smectic C phase has been observed for nonsymmetric dimers.[15,16] More recently, a rather similar texture has been reported for a smectic phase exhibited by a bent methylene linked symmetric liquid crystal dimer[31] and an alternating smectic C phase was proposed although this assignment could not be verified by X-ray diffraction due to the monotropic nature of the phase. The X-ray diffraction pattern of the smectic phase exhibited by 4-*m*5*m*-4 contained a weak reflection in the small angle region implying a layered structure and a broad peak in the wide angle indicating a liquid-like arrangement of the molecules within the layers. The layer spacing was approximately 33 Å which is half that of the estimated all-*trans* molecular length of the most extended conformation of 67 Å, see Fig. 10. Fig. 11 shows a schematic representation of the local molecular arrangement within an alternating smectic C phase for which the ratio of the layer spacing to the molecular length, *d*/*l*, is approximately 0.5. The mesogenic units are tilted with respect to the layer normals but the tilt direction alternates passing from one layer to another such that the global tilt angle is zero. This assignment is consistent with both the observed optical textures, see Fig. 9, and the value of $\Delta S/R$ for the combined smectic–nematic–isotropic transition. The phase structure is analogous to that of the alternating phase reported by Watanabe and co-workers for the semi-flexible main chain liquid crystal polymers.[5–9] Presumably the driving force for the formation of this phase by the tetramers is the ability of such bent molecules to pack efficiently into the structure shown in Fig. 11. It is interesting to note that the terminal chains overlap the inner spacer in this arrangement shown in Fig. 11 and thus the maximum length of the terminal chain that can be accommodated is half the inner spacer length; this is now under further investigation. Fig. 10 shows also a horseshoe-shaped conformation of 4-*m*5*m*-4 which energetically is as favourable as the extended conformation. In a liquid crystal environment, however, the field would presumably preferentially, but not exclusively, select the more extended conformation. In addition, it is not clear how these horseshoe conformations could be arranged into a structure with the experimentally observed *d*/*l* ratio of 0.5.

On cooling the isotropic phase of 6-*m*5*m*-6 a nematic texture develops which changes immediately to give regions of truncated focal-conic fan and homeotropic textures, see Fig. 12, implying that this is not an alternating structure. This phase transition supercools by just 1 °C, see Fig. 8. The phase is viscous but can be sheared. The wide angle region of the X-ray diffraction pattern contains a number of strong reflections, see Fig. 13. This would indicate a crystalline rather than a highly ordered smectic phase and the optical texture is very similar to that observed for the crystal B phase. The X-ray diffraction pattern does not support this assignment; specifically the strong peaks observed in the range 9–12° would not be present for a crystal B phase. We note, however, the strong similarity in the appearance of this pattern to that of the B_3 phase.[1] The optical textures of the phases exhibited by 8-*m*5*m*-8, 9-*m*5*m*-9 and 10-*m*5*m*-10 are similar to that seen for 6-*m*5*m*-6 but the monotropic nature of these phases precluded their study using X-ray diffraction. Each of these homologues also

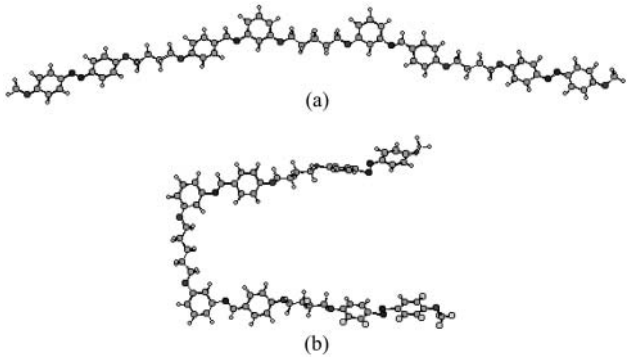

Fig. 10 The molecular shapes of 4-*m*5*m*-4 with the spacers in the all-*trans* conformation; (a) the most extended conformation and (b) the horseshoe conformation.

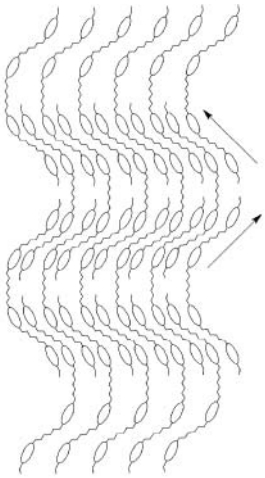

Fig. 11 Sketch of the possible molecular arrangement of 4-*m*5*m*-4 in an alternating smectic C phase.

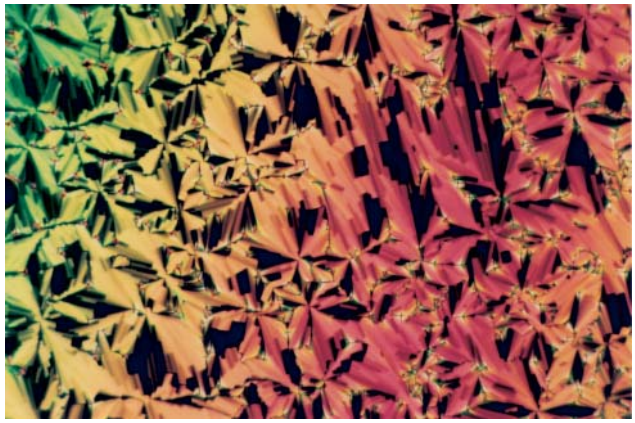

Fig. 12 The truncated fan texture exhibited by the lower temperature phase of 6-*m*5*m*-6 (152 °C).

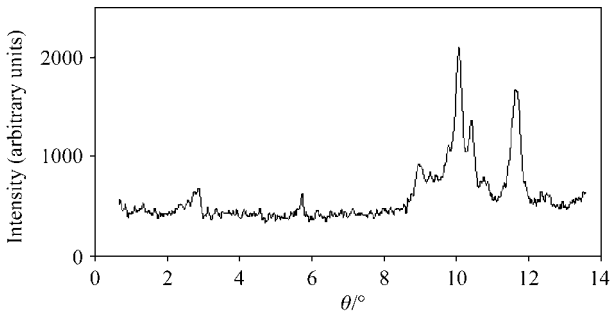

Fig. 13 X-Ray diffraction pattern for the lower temperature phase of 6-*m*5*m*-6 (148 °C).

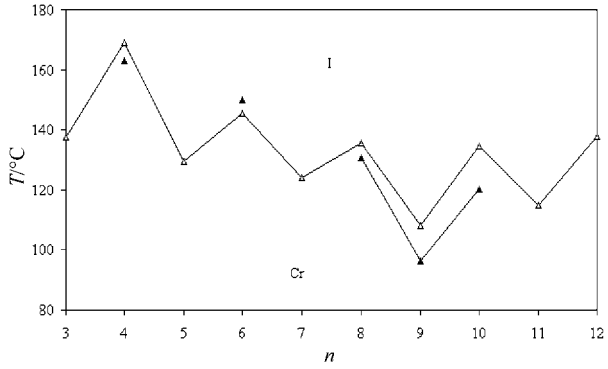

Fig. 14 The dependence of the transition temperatures on the number of methylene units, *n*, in the outer flexible alkyl spacers for the *n*-*m*5*m*-*n* series. △ indicates the melting point and ▲ the mesophase–nematic–isotropic transition temperatures.

exhibits a fleeting nematic phase. The combined entropy change at the clearing transition for these four homologues is entirely consistent with a smectic–nematic–isotropic transition although the X-ray diffraction pattern shown in Fig. 13 precludes such an assignment. The ability of the phase to shear combined with the low transitional entropy indicate that this must be a highly disordered crystal phase. It is noteworthy that the combined entropy change does not depend on the parity of *n* quite unlike the behaviour seen for the *n*-*p*5*p*-*n* and *n*-*p*5*m*-*n* series. It would be unwise to speculate further on the molecular organisation within the mesophase exhibited by 6-*m*5*m*-6, 8-*m*5*m*-8, 9-*m*5*m*-9 and 10-*m*5*m*-10 and further structural studies are now required.

The dependence of the transition temperatures on *n* for the *n*-*m*5*m*-*n* series is shown in Fig. 14. The melting points again exhibit a pronounced alternation as *n* is increased with even members having the higher values. The difference between the clearing temperatures of 8-*m*5*m*-8, and 9-*m*5*m*-9 and between 9-*m*5*m*-9 and 10-*m*5*m*-10 are larger than those between the corresponding members of either the *n*-*p*5*p*-*n* or *n*-*p*5*m*-*n* series. This reflects, at least in part, that the clearing temperature of the even members of the *n*-*m*5*m*-*n* series decrease less quickly than those of the even members in either the *n*-*p*5*p*-*n* or *n*-*p*5*m*-*n* series on increasing *n*. Thus, the odd–even effect is apparently not attenuated as rapidly. We will return to this observation later.

Comparison of the series

The dependence of the melting points on the number of methylene units in the outer flexible alkyl spacers, *n*, is shown for all three tetrameric series in Fig. 15. As we have already seen, the melting points of each series depend critically on the length and parity of these spacers and pronounced alternations in the melting point are observed on increasing *n*. Similar behaviour has been reported on increasing the length of alkyl spacers in liquid crystal tetramers containing an even-membered inner spacer,[26] trimers[24] and nematic dimers[28,32] but not for smectic dimers.[28] This behaviour may be interpreted in two ways. It may indicate that the change in the conformation statistical weights of the spacers on melting into a nematic phase is small for even-membered spacers but large for odd-membered spacers. An alternative explanation considers enthalpic effects and at the root of the dramatic odd–even effect is possibly the difficulty that the odd-membered compounds, with their bent molecular shapes, experience in packing efficiently into a crystalline structure as compared with the more linear even-membered compounds, see Fig. 16 and 17. This latter view is supported by the trend in the melting points on changing the molecular structure. Thus, for any given value of *n*, *n*-*p*5*p*-*n* exhibits a higher melting point than *n*-*p*5*m*-*n* which in turn is higher than that shown by *n*-*m*5*m*-*n*. It is interesting to note that the difference in melting point between *n*-*p*5*p*-*n* and *n*-*p*5*m*-*n* is larger than that between *n*-*p*5*m*-*n* and *n*-*m*5*m*-*n*. This strongly suggests that molecular shape is an important parameter in determining the melting point and that there is a larger difference in shape between *n*-*p*5*p*-*n* and *n*-*p*5*m*-*n* than between *n*-*p*5*m*-*n* and *n*-*m*5*m*-*n*.

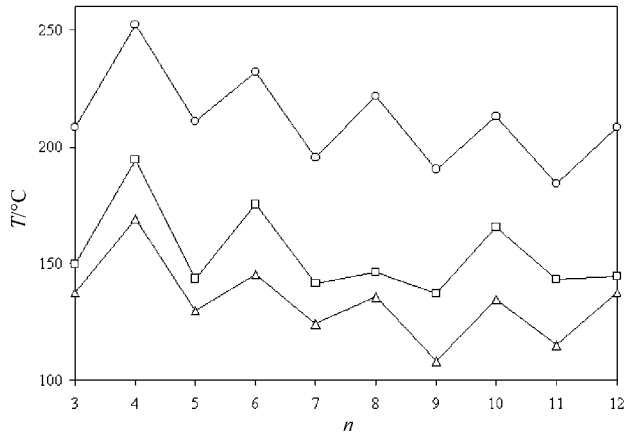

Fig. 15 The dependence of the melting points on the number of methylene units, *n*, in the outer flexible alkyl spacers for the *n*-*p*5*p*-*n* series (○), the *n*-*p*5*m*-*n* series (□) and the *n*-*m*5*m*-*n* series (△).

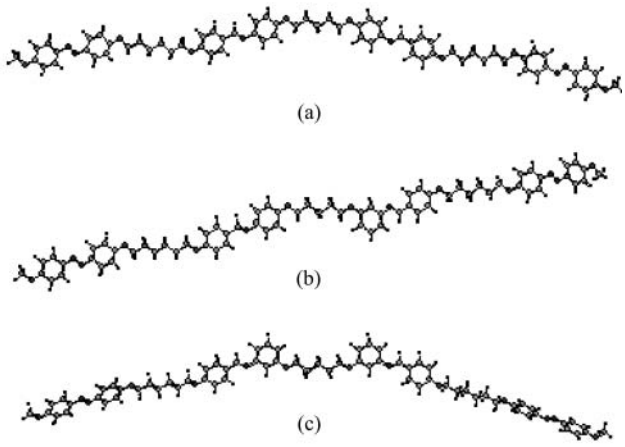

Fig. 16 The extended molecular shapes of (a) 6-*p*5*p*-6, (b) 6-*p*5*m*-6 and (c) 6-*m*5*m*-6 with the spacers in the all-*trans* conformation.

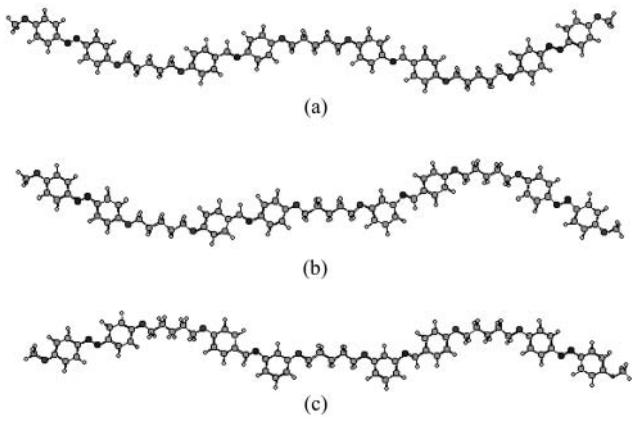

Fig. 17 The extended molecular shapes of (a) 5-*p*5*p*-5, (b) 5-*p*5*m*-5 and (c) 5-*m*5*m*-5 with the spacers in the all-*trans* conformation.

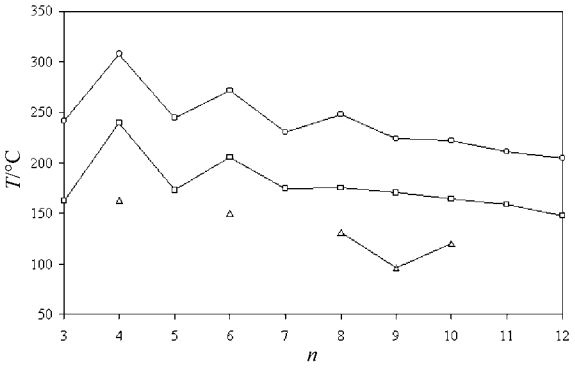

Fig. 18 The dependence of the clearing temperatures on the number of methylene units, *n*, in the outer flexible alkyl spacers for the *n-p5p-n* series (○), the *n-p5m-n* series (□) and the *n-m5m-n* series (△).

Fig. 18 compares the clearing temperatures of the *n-p5p-n*, *n-p5m-n*, and *n-m5m-n* series. For any given value of *n*, *n-p5p-n* has the highest clearing temperature then *n-p5m-n* and *n-m5m-n* exhibits the lowest clearing temperature. This trend presumably reflects the enhanced shape anisotropy on passing from the *n-m5m-n* to the *n-p5m-n* and *n-p5p-n* structures, see Fig. 16 and 17. Here we consider only the most extended conformations of each compound as these will be preferentially selected by the nematic field.

Fig. 4 shows the comparison of the entropy changes associated with the clearing transition for the three series. For a given value of *n* the clearing entropy exhibited by a member of the *n-p5p-n* series is higher than that shown by a member of the *n-p5m-n* series. This observation is difficult to interpret unambiguously although presumably reflects, at least in part, the increase in the biaxiality of the molecules.[33] The exception to this trend are the decyl homologues for which $\Delta S_{NI}/R$ for 10-*p5p*-10 is lower than that of 10-*p5m*-10. We have commented already, however, that $\Delta S_{NI}/R$ for 10-*p5p*-10 is lower than expected and that this may be attributed to the close proximity of the melting transition. The values of $\Delta S_{NI}/R$ listed in Tables 1 and 2 are considerably larger than those exhibited by conventional low molar mass mesogens, odd-membered dimers and odd-membered trimers, but do fit the emerging trend that $\Delta S_{NI}/R$ increases on passing from the monomer, to the dimer, trimer and tetramer.[24,26] It has been argued that these values should be scaled according to the number of mesogenic groups and indeed such a scaling is routinely performed when analysing either enthalpic or entropic data for semi-flexible main chain liquid crystal polymers. Thus, the scaled value of $\Delta S_{NI}/R$ for 5-*p5p*-5 (*i.e.* $[\Delta S_{NI}/R]/4 = 0.46$) is comparable in magnitude to that of a trimer containing pentamethylene spacers (*i.e.* $[\Delta S_{NI}/R] = 0.38$)[24] although we note that the mesogenic units in the trimer and tetramer are different. Work is now in progress to establish for chemically comparable systems how $\Delta S_{NI}/R$ scales with the number of mesogenic units and spacers and whether this depends on the parity of the spacer.

We have seen in Fig. 18 and 4 that the transitional properties of the *n-p5p-n* and *n-p5m-n* series depend critically on the length and parity of the spacer in a manner strongly resembling that seen for the transitional properties of dimers, trimers and semi-flexible main chain liquid crystal polymers. As we noted in the Introduction, such behaviour is most often attributed to the dependence of the molecular shape on the parity of the spacer considered in the all-*trans* conformation. Thus, in an even-membered dimer the mesogenic units are antiparallel whereas in an odd-membered dimer they are inclined at some angle with respect to each other. This more linear structure for even-membered dimers is then considered to be more compatible with the molecular organisation found in the nematic phase than that of the bent odd-membered dimers and it is this greater compatibility which results in, for example, the higher values of $\Delta S_{NI}/R$ found for the even-members. This interpretation, however, completely neglects the flexibility of the spacer and a more realistic interpretation of the dependence of the transitional properties on the parity of the spacer must certainly include a wide range of conformations and not just the all-*trans* conformation. Such a model has been developed[13] and shows that in the isotropic phase approximately half the conformers of an even-membered dimer are essentially linear compared to only 10% of the conformers of an odd-membered dimer. At the transition to the nematic phase the synergy that exists between conformational and orientational order ensures that for even-membered dimers many of the bent conformers are converted to a linear form so enhancing the orientational order of the nematic phase. This increases $\Delta S_{NI}/R$ relative to what would be expected for a monomer. For an odd-membered dimer, however, the difference in free energy between the bent and linear conformers is too large for the orientational order of the nematic phase to convert bent into linear conformers. Thus, odd-membered dimers exhibit smaller values of $\Delta S_{NI}/R$ than even-membered dimers. For tetramers we now have three spacers to consider, one of which is always odd for these particular series. It would seem reasonable to assume that this model would also successfully predict the transitional properties of the tetramers. The odd–even effect shown by the nematic–isotropic transition temperatures for the *n-p5p-n* and *n-p5m-n* series attenuates on increasing *n*, see Fig. 18, whereas that shown by $\Delta S_{NI}/R$ do not, see Fig. 4. This is also archetypal behaviour for dimers and presumably reflects that on increasing the spacer length the greater number of available conformations means that the average shapes of the molecules, and hence the interaction strength parameters between them, become more similar. Thus, the alternation in T_{NI} attenuates but there will still be a marked difference in the conformational distributions of the spacers giving rise to the odd–even effect seen for $\Delta S_{NI}/R$. This explanation also accounts for the more rapid attenuation of the alternation in T_{NI} for the *n-p5m-n* series. Thus, the change in substitution pattern around the inner two mesogenic units serves to reduce the difference in the shapes of the odd and even membered compound, see Fig. 16 and 17. On passing to the *n-m5m-n* series the difference in the shape between the odd and even members is reinforced and the alternation in T_{NI} becomes more pronounced. It is not possible to comment on the trend in clearing entropies because for the *n-m5m-n* series this represents a combined transition.

Finally, it is apparent that as we pass from the *n-p5p-n* series to the *n-p5m-n* and *n-m5m-n* series there is an increasing tendency to exhibit higher ordered mesophases. This strongly suggests that the more bent molecules can pack more efficiently and in a manner reminiscent of that observed for certain semi-flexible main chain liquid crystal polymers.[5–9]

References

1 G. Pelzl, S. Diele and W. Weissflog, *Adv. Mater.*, 1999, **11**, 707.
2 T. Niori, T. Sekine, J. Watanabe, T. Furukawa and H. Takezoe, *J. Mater. Chem.*, 1996, **6**, 1231.
3 H. R. Brand, P. E. Cladis and H. Pleiner, *Eur. Phys. J. B*, 1998, **6**, 347.
4 T. Sekine, T. Niori, J. Watanabe, T. Furukawa, S. W. Choi and H. Takezoe, *J. Mater. Chem.*, 1997, **7**, 1307.
5 J. Watanabe and M. Hayashi, *Macromol.*, 1988, **21**, 278.
6 J. Watanabe and M. Hayashi, *Macromol.*, 1989, **22**, 4083.
7 J. Watanabe and S. J. Kinoshita, *J. Phys. II*, 1992, **2**, 1237.
8 J. Watanabe, M. Hayashi and M. Morita, *Mol. Cryst. Liq. Cryst.*, 1994, **254**, 221.
9 M. Tokita, K. Osada and J. Watanabe, *Liq. Cryst.*, 1998, **24**, 477.
10 H. Finkelmann, in *Thermotropic Liquid Crystals*, ed. G. W. Gray, 1987, Wiley, Chichester, Ch. 6.
11 C. K. Ober, J.-I. Jin and R. W. Lenz, *Adv. Poly. Sci.*, 1984, **59**, 103.
12 C. T. Imrie, *Struct. Bond.*, 1999, **95**, 149.
13 C. T. Imrie and G. R. Luckhurst, *Liquid Crystal Dimers and*

Oligomers, in *Handbook of Liquid Crystals*, ed. D. Demus, J. W. Goodby, G. W. Gray, H. W. Spiess and V. Vill, Vol. 2B, 1998, Wiley-VCH, Weinheim, p. 801.
14 G. R. Luckhurst, *Macromol. Symp.*, 1995, **96**, 1.
15 G. S. Attard, S. Garnett, C. G. Hickman, C. T. Imrie and L. Taylor, *Liq. Cryst.*, 1990, **7**, 495.
16 G. S. Attard, R. W. Date, C. T. Imrie, G. R. Luckhurst, S. J. Roskilly, J. M. Seddon and L. Taylor, *Liq. Cryst.*, 1994, **16**, 529.
17 H. Furuya, K. Asahi and A. Abe, *Polym. J*, 1986, **18**, 779.
18 G. S. Attard and C. T. Imrie, *Liq. Cryst.*, 1989, **6**, 387.
19 R. Centore, A. Roviello and A. Sirigu, *Mol. Cryst. Liq. Cryst.*, 1990, **182B**, 233.
20 T. Ikeda, T. Miyamoto, S. Kurihara, M. Tsukada and S. Tazuke, *Mol. Cryst. Liq. Cryst.*, 1990, **182B**, 357.
21 A. T. M. Marcelis, A. Koudijs and E. J. R. Sudhölter, *Liq. Cryst.*, 1996, **21**, 87.
22 A. T. M. Marcelis, A. Koudijs and E. J. R. Sudhölter, *Liq. Cryst.*, 1995, **18**, 851.
23 N. V. Tsvetkov, V. V. Zuev and V. N. Tsvetkov, *Liq. Cryst.*, 1997, **22**, 245.
24 C. T. Imrie and G. R. Luckhurst, *J. Mater. Chem.*, 1998, **8**, 1339.
25 A. T. M. Marcelis, A. Koudijs and E. J. R. Sudhölter, *Mol. Cryst. Liq. Cryst.*, 1999, **330**, 1289.
26 C. T. Imrie, D. Stewart, C. Remy, D. W. Christie, I. W. Hamley and R. Harding, *J. Mater. Chem.*, 1999, **9**, 2321.
27 C. T. Imrie, F. E. Karasz and G. S. Attard, *Macromol.*, 1992, **25**, 1278.
28 R. W. Date, C. T. Imrie, G. R. Luckhurst and J. M. Seddon, *Liq. Cryst.*, 1992, **12**, 203.
29 W. L. McMillan, *Phys. Rev. A.*, 1971, **4**, 1238.
30 J. Watanabe, H. Komura and T. Niori, *Liq. Cryst.*, 1993, **13**, 455.
31 P. A. Henderson, O. Niemeyer and C. T. Imrie, *Liq. Cryst.*, 2001, **28**, 463.
32 J. W. Emsley, G. R. Luckhurst, G. N. Shilstone and I. Sage, *Mol. Cryst. Liq. Cryst.*, 1984, **102**, 223.
33 C. T. Imrie, *Liq. Cryst.*, 1989, **6**, 391.